

PAPER • OPEN ACCESS

## Growth and optical properties of GaPN/GaP heterostructure nanowire array

To cite this article: O Yu Koval *et al* 2019 *J. Phys.: Conf. Ser.* **1400** 055036

View the [article online](#) for updates and enhancements.

You may also like

- [Controllable antiphase domain density in dilute nitride GaPN/GaP heterostructures on silicon](#)  
V.V. Fedorov, A.D. Bolshakov, O.Yu. Koval *et al.*
- [GaPN/GaP nanowire-polymer matrix: photoluminescence study](#)  
O Yu Koval, V V Fedorov, A D Bolshakov *et al.*
- [Improved crystallinity of GaP-based dilute nitride alloys by proton/electron irradiation and rapid thermal annealing](#)  
Keisuke Yamane, Ryo Futamura, Shigeto Genjo *et al.*



**ECS**  
The  
Electrochemical  
Society  
Advancing solid state &  
electrochemical science & technology

**DISCOVER**  
how sustainability  
intersects with  
electrochemistry & solid  
state science research

# Growth and optical properties of GaPN/GaP heterostructure nanowire array

O Yu Koval<sup>1</sup>, G A Sapunov<sup>1</sup>, V V Fedorov<sup>1</sup> and I S Mukhin<sup>1,2</sup>

<sup>1</sup> St. Petersburg Academic University, 194021, St. Petersburg, Russia

<sup>2</sup> ITMO University, 197101, St. Petersburg

**Abstract.** The study is devoted to synthesis and investigation of the optical properties of GaPN/GaP nanowire (NW) arrays grown on Si substrate (111) with plasma-assisted molecular beam epitaxy (PA-MBE). First, we demonstrate the growth of axial GaPN/GaP and GaP NW heterostructures. The morphology of GaP and GaPN/GaP NW arrays was investigated with scanning electron microscopy (SEM) to show that at low growth fluxes of activated nitrogen self-catalytic growth regime and nanowires morphology are preserved. Raman spectroscopy was used for investigation of phonon spectra features. Optical properties of the GaPN NW arrays were determined at room temperature with photoluminescence (PL) spectroscopy. Analysis of both Raman spectroscopy and PL results allowed to analyze the GaPN/GaP NWs chemical composition. Dilution of GaP NWs with N allows to significantly increase PL intensity and obtain broad PL signal in the optical spectral region demonstrating the potential of GaPN NWs for future nano-optoelectronics and photonics.

## 1. Introduction

Gallium Phosphide (GaP) is an indirect-gap semiconductor material with a bandgap of 2.26 eV [1]. Dilution of III-V compounds, in particular, gallium phosphide, with isoelectronic nitrogen impurity (N) is widely used to increase the radiative efficiency of the material and therefore makes it suitable for use in highly-efficient light emitting devices operating in the visible and IR spectral range [2]. At very low N concentrations ( $\sim 10^{16} \text{ cm}^{-3}$ ), the isolated impurity atom acts as an isoelectronic center in GaP [3], with highly localized energy level slightly below the minimum of the GaP conduction band. Since the 80s this material is frequently used for light emitting diodes (LED) of yellow and green color, however, it demonstrates lower quantum efficiencies in compare to the direct bandgap III-V alloys. Higher concentrations of N in diluted III-V compounds were achieved only with development of growth techniques, such as molecular beam epitaxy with N plasma activation (PA-MBE). Further incorporation of N atoms into  $\text{GaP}_{1-x}\text{N}_x$  alloys with ( $x > 0.43\%$ ) leads to the bandgap shrinkage and indirect to direct bandgap transition and, which allows the realization of efficient LEDs operating in a yellow spectral region. Unique shape of the semiconductor nanowires (NWs) promotes efficient relaxation of mechanical strains in mismatched systems [4] and allows to circumvent the miscibility gap between different materials [5]. That is why GaPN NWs grown on Si substrate is the object of high interest due to promising perspectives for the future opto-nanoelectronics [6]. The purpose of this work is Raman and photoluminescence (PL) spectroscopy characterization of the phonon spectra and optical properties of GaPN/GaP NWs.



## 2. Experimental

GaPN/GaP NW array was synthesized on the silicon substrate (111) by PA-MBE in Veeco GEN-III MBE setup with the use of Riber valved RF-plasma (13.56 MHz) source of activated nitrogen [7]. Silicon (111) wafers cleaned according to the modified Shiraki method were used as substrates. The synthesis of silicon oxide on the substrate surface was performed by boiling in 35% nitric acid water solution. After loading and degassing the substrate was annealed at 800°C, which is lower than the temperature required to thermally deoxidize silicon. The growth temperature was measured by both thermocouple and pyrometer and was equal 630°C during the growth process. Ga flux was kept constant and equivalent to the 0.4 ML/s growth rate of planar GaP/Si(111), calibrated by reflection high energy electron diffraction (RHEED), and corresponds to Ga beam equivalent pressure (BEP) equal to the  $8 \times 10^{-8}$  Torr. The synthesized sample represent GaPN/GaP heterostructured NWs consisting from GaPN segment grown on GaP stem. The growth time of the GaP stem and GaPN segment was equal. P/Ga BEP ratio was kept constant during the growth of GaP and GaPN and equal 18. The growth was not interrupted during the plasma ignition. As a reference, GaP NWs was grown at the same growth conditions but without nitrogen flux. To study the effect of N atom incorporation on the optical properties of pure and nitrogen-diluted phosphide NWs Raman and PL spectroscopy were used. The Raman scattering (RS) and PL spectra were obtained in backscattering geometry at room temperature (300K) on a Horiba LabRam HR800 Raman spectrometer equipped with a CCD detector. The laser at excitation wavelength  $\lambda = 532$  nm (2.331 eV) was used. The structure and morphology were studied using scanning electron microscopy (SEM) (Zeiss SUPRA 25-30-63).

## 3. Results

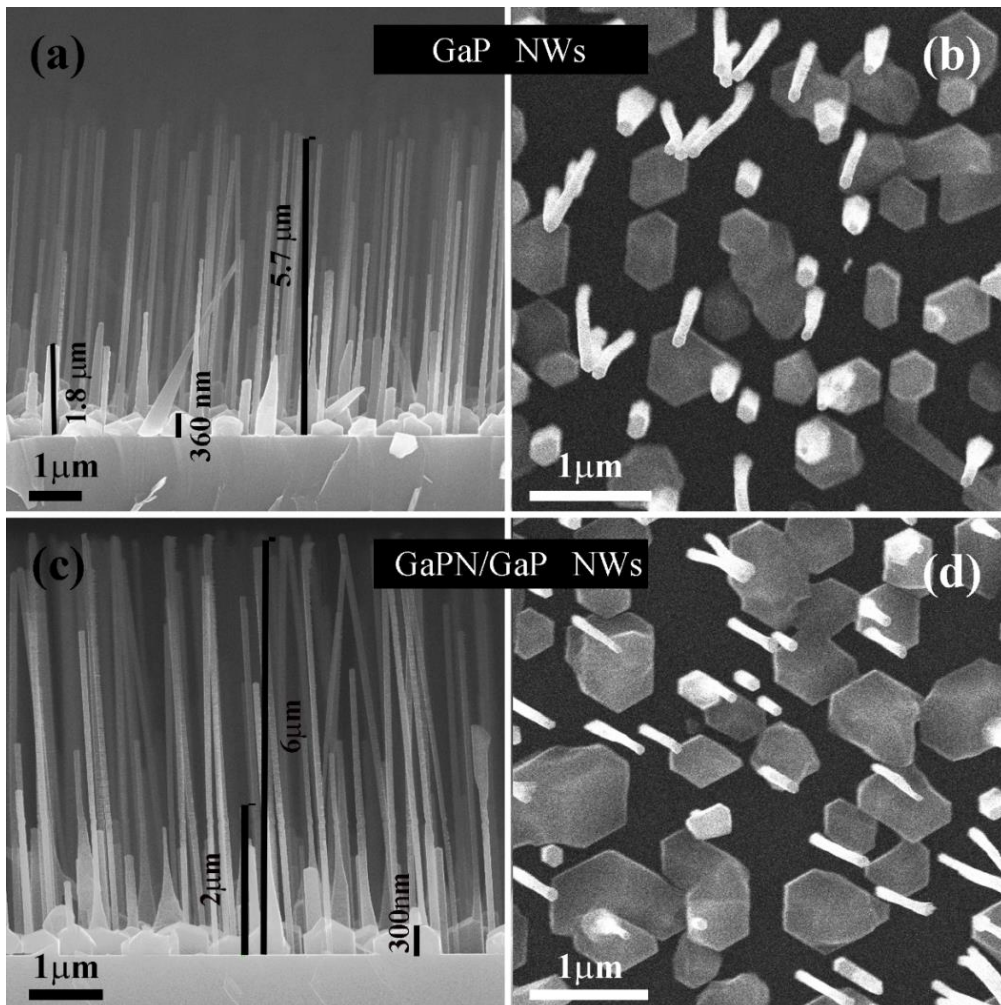
### 3.1. The growth

Figure 1 shows SEM images of the studied epitaxial NW arrays. Both vertical NWs (with surface density  $\sim 1.5 \mu\text{m}^{-1}$ ) and 3D- nanoscale islands (surface dens  $\sim 1 \mu\text{m}^{-1}$ ) with flat (111) facets are formed at chosen growth conditions. We assume that their formation corresponds to GaP nucleation with (111)B and (111)A polarity accordingly. As can see in Figure 1 (b, d), the NWs and 3D- islands are hexagonal in their cross-sections, indicating that they are following the Si(111) substrate crystallographic orientation. The NWs are rather uniform in size for both studied samples and have the length of about 5.7–6  $\mu\text{m}$ . The average diameter of single NW  $\sim 100$  nm (Figure 1 a, c). The average height of the 3D islands is about  $\sim 300$ -350nm. Comparing both samples, we conclude that used nitrogen flux does not affect the nanostructure morphology and preserves self-catalytic growth. According to the reflection high-energy electron diffraction (RHEED) pattern observed at the end of the growth (not presented here), NWs exhibit zinc-blend (ZB) structure with a rotational twinning in [111] growth direction typical for GaP NWs, however weak intensity WZ pattern was also registered [8].

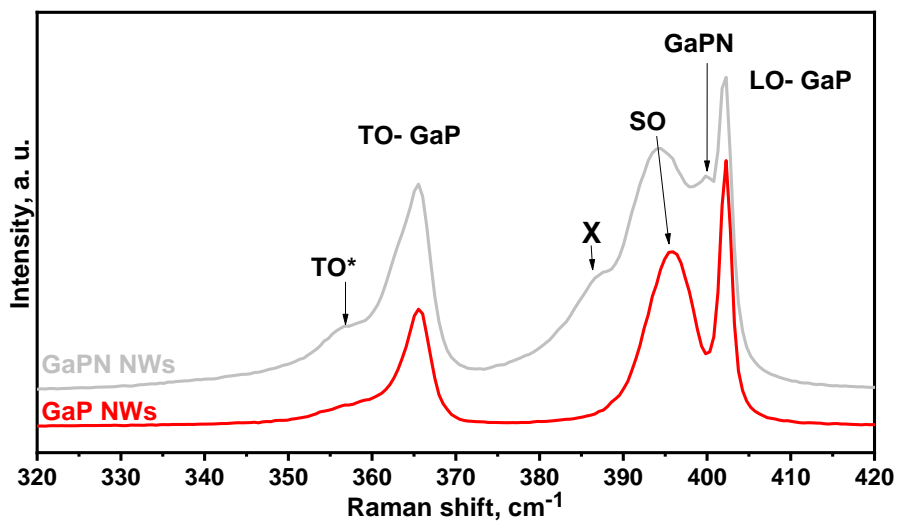
### 3.2. Raman spectroscopy study

Figure 2 presents Raman spectra from GaP and GaPN/GaP NW arrays measured at backscattering geometry. The samples spectra possess 3 pronounced bands, quite common for NWs geometry [9], namely: the transverse (TO-), longitudinal (LO-) phonon modes corresponding to the zone-center ( $\Gamma$ ) optical phonons in ZB GaP and surface optical phonon (SO) mode, that can be activated via breakdown of translational symmetry at surfaces. The observed modes are located at 365, 402 and 394  $\text{cm}^{-1}$ , respectively [10, 11].

The additional mode at 387  $\text{cm}^{-1}$  (labelled as X) is also observed in the Raman spectra of the planar GaPN epilayer, in accordance with previous researches [9, 12]. The activation of this mode can be explained by relaxation of the momentum conservation rules as a result of the translational symmetry breaking by incorporation and clustering of N atom into the GaP matrix.



**Figure 1.** SEM micrograph of the high-density NWs grown homogeneously on Si[111] substrates, where: *a* and *b* – SEM images of pure GaP heterostructure NWs array, *c* and *d* SEM images of GaPN/GaP NWs array.



**Figure 2.** Room-temperature RS spectra measured from GaP and GaPN/GaP NWs arrays.

The appearance of Raman band at the low-energy side of the TO mode was previously observed in III-V NWs with WZ inclusions [9, 13]. The position of the TO\* peak in our sample is indeed very close to the energy of the TO phonons in GaP at the critical point L on the edge of the Brillion zone – TO (L). Alternatively, additional modes could be activated due to translational symmetry breaking caused by the formation of either planar (e.g., twinning planes and mixed WZ/ZB segments) or point defects that relaxes Raman selection rules, for example, peak at  $400\text{ cm}^{-1}$ , which can be attributed to LO mode of GaPN alloy [14].

### 3.3. Photoluminescence study

PL spectra of the studied heterostructured vertical GaPN/GaP NWs array obtained at 300 K demonstrate the presence of typical for GaPN alloys broadband PL signal [3, 15] (Figure 3). Investigation of the pure GaP NWs array demonstrates the absence of the PL signal indicating that N incorporation contributes to the increase in the quantum efficiency of the PL, more likely due to the indirect-to-direct band structure transition. The emission originates from radiative recombination at N-related localized states [16 - 18]. Broad PL signal is common for the highly mismatched alloys such as a GaPN and additionally, can be broadened due to the uncontrollable variation of chemical composition in NWs array due to their size dispersion, as N incorporation can be sensitive to the NW dimensions [19] of synthesized NW sample. The central position of PL signal is located at 600 nm and to evidence of nitrogen concentration at  $\sim 0.5\%$  [20].

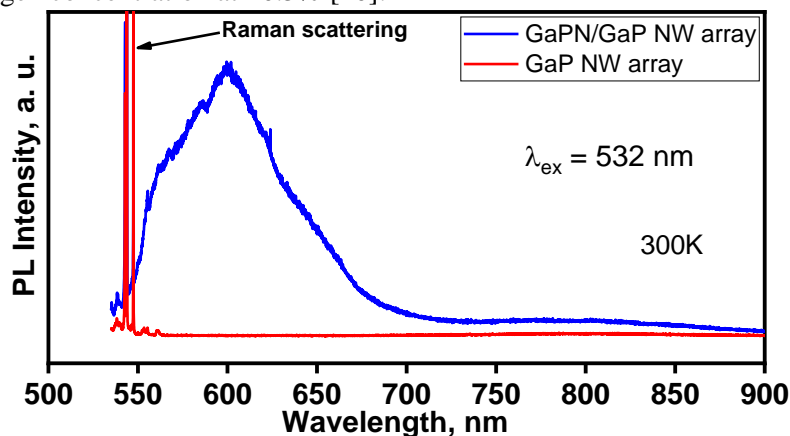


**Figure 3.** PL emission of GaPN/GaP (blue line) and GaP (red line) NW arrays performed at room temperature.

## 4. Conclusions

In conclusion, the vertical self-catalyzed axially heterostructured GaPN/GaP and pure GaP epitaxial NW arrays were grown on Si (111) by nitrogen PA-MBE. It is demonstrated experimentally that incorporation of a small nitrogen fraction does not change the NW morphology and preserves self-catalytic growth despite the presence of N promoting self-induced GaP NWs growth.

Also, we have shown that GaPN NWs demonstrate the appearance of wide PL emission signal with the maximum in the visible spectral range. The Raman scattering peaks, which can be attributed to the GaP-like LO and TO phonon modes are found to dominate the  $350\text{--}410\text{ cm}^{-1}$  spectral range. Two additional peaks at  $355, 390\text{ cm}^{-1}$  are also registered at Raman spectra of both samples and could be attributed to zone-edge TO phonons and a surface mode, respectively. Two additional peaks, which located at  $386$  and  $400\text{ cm}^{-1}$ , related to the N incorporation appear in GaPN/GaP NWs.

## Acknowledgements

The authors acknowledge support from the Ministry of Science and Higher Education of the Russian Federation (RFMEFI61619X0115).

## References

- [1] Mozharov A M et al. 2016 *Semiconductors* **50**(11) 1521–25
- [2] Bolshakov A D et al. 2018 *Semiconductors* **52**(16) 2088–99
- [3] Dobrovolsky A et al. 2012 *Appl. Phys. Lett.* **101** 163106
- [4] Dubrovskii et al. 2012 *Tech. Phys. Lett.* **38**(4) 311–15
- [5] Bolshakov A D et al. 2017 *Mater. Res. Express* **4**(12) 125027
- [6] Jansson M et al. 2017 *J. Phys. Chem. C* **121**(12) 7047–55
- [7] Bolshakov A D et al. 2018 *Beilstein J. Nanotechnol* **9**(1) 146–54
- [8] Fedorov V V et al. 2018 *Semiconductors* **52**(16) 2092–95
- [9] Dobrovolsky A, et al. 2014 *Appl. Phys. Lett.* **105**(19) 193102
- [10] Zhang Z et al. 2006 *Rare Met.* **25**(3) 253–59
- [11] Hayashi S et al. 1982 *Phys. Rev. B* **26**(12) 7079–82
- [12] Pulzara-Mora A et al. 2006 *Vacuum* **80**(5) 468-74
- [13] Zardo I et al. 2009 *Phys. Rev. B* **80**(24) 245324
- [14] Bolshakov A D et al. 2019 *Cryst. Growth Des.* **19**(8) 4510-20
- [15] Buyanova I A et al. 2001 *Phys.B Condens. Matter* **308** 106–9
- [16] Dobrovolsky A et al. 2012 *Appl. Phys. Lett.* **101**(16) 163106
- [17] Shan W et al. 2000 *Appl. Phys. Lett.* **76**(22) 3251–53
- [18] Kent P R C et al. 2001 *Phys. Rev. B* **64**(11) 115208
- [19] Fedorov V V et al. 2018 *Cryst. Eng. Comm.* **20**(24) 3370–80
- [20] Buyanova I A et al. 2002 *Appl. Phys. Lett.* **80**(10) 1740–42